Inorg. Chem. 1983, 22, 2178-2183

Contribution from the Department of Chemistry,
McMaster University, Hamilton, Ontario L8S 4M1, Canada

Synthesis, Multinuclear Magnetic Resonance, and Raman Study of ^{15}N-Enriched $Xe[N(SO_2F)_2]_2$, an Example of Xenon–Nitrogen Bonding. Solution Behavior of $[^{15}N]$-$F[XeN(SO_2F)_2]_2^+AsF_6^-$

GERHARD A. SCHUMACHER and GARY J. SCHROBILGEN*

Received October 7, 1982

The synthesis of ^{15}N-enriched $Xe[N(SO_2F)_2]_2$ is discussed and ^{15}N and ^{129}Xe NMR evidence for the proposed structure is presented based on the observed ^{129}Xe–^{15}N couplings. The latter couplings arise from three possible isotopic isomers and conclusively demonstrate that the compound contains two equivalent Xe–N bonds. Low-temperature Raman data for the solid compound have been assigned by analogy with $FXeN(SO_2F)_2$ and are consistent with Xe–N bonding in the solid state. The dissociation of ^{15}N-enriched $F[XeN(SO_2F)_2]_2^+AsF_6^-$ in BrF_5 and SO_2ClF solvents has been studied by ^{129}Xe, ^{19}F, and ^{15}N NMR spectroscopy and shown to have a marked dielectric dependence. In SO_2ClF media, the cation is shown to dissociate, giving rise to $Xe[N(SO_2F)_2]_2$. Shielding anisotropy has been shown to play a dominant role in the relaxation of ^{129}Xe in $FXeN(SO_2F)_2$ at high applied field strengths.

Introduction

It is only recently that a compound containing a xenon–nitrogen bond has been definitively characterized. The first such example was synthesized by DesMarteau and LeBlond,[1] namely, $FXeN(SO_2F)_2$, and has recently been fully characterized by X-ray crystallography and multinuclear NMR and Raman spectroscopy by Schrobilgen et al.[2,3] and shown to contain an Xe–N bond (2.200 (3) Å). Prior to the synthesis and characterization of this compound only Xe—F, Xe—O, and Xe═O bonds had been shown to exist.

Since the first report of $FXeN(SO_2F)_2$, it has been shown that the compound forms a stable adduct with AsF_5, yielding what is tentatively formulated as $F[XeN(SO_2F)_2]_2^+AsF_6^-$,[4] in which the two xenon atoms are thought to be fluorine bridged as in the $Xe_2F_3^+$ [5] and $Kr_2F_3^+$ [6] cations.

Previous work has demonstrated the importance of a multinuclear approach to NMR in the characterization of noble-gas compounds.[7,8] The present work reports the preparation of $Xe[N(SO_2F)_2]_2$ and its characterization using multinuclear magnetic resonance spectroscopy of isotopically (^{15}N) enriched compounds. The compound is shown to be the first example of xenon bonded to two nitrogen atoms. The Raman spectrum of the solid compound is assigned on the basis of this interpretation. In the course of this study, an independent report of the preparations of nonenriched $Xe[N(SO_2F)_2]_2$ has appeared;[4] the present study, however, represents the first definitive characterization of Xe–N bonds for this compound.

The fluorine-bridged cation $F[XeN(SO_2F)_2]_2^+$ is apparently dissociated in BrF_5 solution.[4] The present study has reexamined these solutions and shown that $Xe[N(SO_2F)_2]_2$ is also involved in the complex dissociative equilibria exhibited by $F[XeN(SO_2F)_2]_2^+$ in SO_2ClF solvent.

Results and Discussion

NMR Spectroscopy. $[^{15}N]$-$Xe[N(SO_2F)_2]_2$. Solutions of $[^{15}N]$-$Xe[N(SO_2F)_2]_2$ ($[^{15}N]$ denotes ^{15}N enrichment) in SO_2ClF were studied by ^{129}Xe and ^{15}N NMR spectroscopy at −40 °C. The ^{129}Xe spectrum consisted of a multiline spectrum at −2257 ppm and is depicted in Figure 1. The multiplicity arises from the series of isotopic isomers $(FO_2S)_2{}^{15}NXe{}^{15}N(SO_2F)_2$ (triplet), $(FO_2S)_2{}^{14}NXe{}^{15}N(SO_2F)_2$ (doublet), and $(FO_2S)_2{}^{14}NXe{}^{14}N(SO_2F)_2$ (singlet). The overlap between the respective triplet, doublet, and singlet results in a five-line spectrum having the relative line intensities 1:9.3:23.7:9.3:1 at 30.0 atom % ^{15}N enrichment. The splitting pattern is conclusive proof of two equivalent nitrogen atoms spin coupled to xenon. The magnitude of the coupling constant $J_{^{129}Xe-^{15}N}$ compared to that of $FXeN(SO_2F)_2$ (307 Hz) is 259 Hz. A previous assessment of the nature of xenon bonding in solution for $FXeN(SO_2F)_2$ using arguments based on reduced coupling constants, $^1K_{Xe-N}$ (Table I, footnote *c*), has ruled out fluxional structures involving both nitrogen and/or oxygen bonding to xenon.[2,3] The ^{129}Xe–^{15}N coupling in $Xe[N(SO_2F)_2]_2$ when compared to that of $FXeN(SO_2F)_2$ must also be assessed as a one-bond Xe–N coupling. The smaller size of $^1K_{Xe-N}$ in the bis compound suggests less sulfur–nitrogen π bonding, resulting in lower s-electron densities at the nitrogen nuclei. Although Xe–N bonds somewhat shorter and more covalent than in $FXeN(SO_2F)_2$ should result, the s-electron density at the xenon nucleus should be little affected as σ-bonding is primarily through the 5p orbitals of xenon. If the Fermi contact mechanism is assumed to be dominant for Xe–N spin–spin coupling, the relative magnitudes of $^1K_{Xe-N}$ values in $FXeN(SO_2F)_2$ and $Xe[N(SO_2F)_2]_2$ reflect the anticipated relative s-electron density changes at the xenon and nitrogen nuclei in these compounds.

The increase in covalent character of the Xe–N bonds of the bis compound is also reflected in the low-frequency position of the ^{129}Xe chemical shift when compared with that of the mono compound. In fact, $Xe[N(SO_2F)_2]_2$ represents the lowest frequency (most shielded) chemically bound xenon environment reported to date.[9] The ^{129}Xe chemical shift trend for XeF_2, $FXeN(SO_2F)_2$, and $Xe[N(SO_2F)_2]_2$ is analogous to that observed over the series XeF_2, FXeL, and XeL_2, where L = OSO_2F and $OTeF_5$. These trends may be regarded, in valence bond terms, as arising from contributions that decrease in the series $F-Xe^+F^-$, $F^-Xe^+L^-$, and $L-Xe^+L^-$ with increasing number of the less electronegative ligand L. The low-frequency position of $N(SO_2F)_2$ compounds of xenon(II) when compared to those of their F, $OTeF_5$, and OSO_2F cogeners is consistent

---

[1] LeBlond, R. D.; DesMarteau., D. D. *J. Chem. Soc., Chem. Commun.* **1974**, 555.

[2] Sawyer, J. F.; Schrobilgen, G. J.; Sutherland, S. J. *J. Chem. Soc., Chem. Commun.* **1982**, 210.

[3] Sawyer, J. F.; Schrobilgen, G. J.; Sutherland, S. J. *Inorg. Chem.* **1982**, *21*, 4064.

[4] DesMarteau, D. D.; LeBlond, R. D.; Hassain, S. F.; Nöthe, D. *J. Am. Chem. Soc.* **1981**, *103*, 7734.

[5] Bartlett, N.; DeBoer, B. G.; Hollander, F. J.; Sladky, F. O.; Templeton, D. H.; Zalkin, A. *Inorg. Chem.* **1974**, *13*, 780.

[6] Gillespie, R. J.; Schrobilgen, G. J. *Inorg. Chem.* **1976**, *15*, 22.

[7] Schrobilgen, G. J.; Holloway, J. H.; Granger, P.; Brevard, C. *Inorg. Chem.* **1978**, *17*, 980.

[8] Schrobilgen, G. J. In "NMR and the Periodic Table"; Harris, R. K., Mann, B. E., Eds.; Academic Press: London, 1978; Chapter 14.

[9] The ^{129}Xe chemical shift of $Xe[N(SO_2CF_3)_2]_2$ has recently been measured (DesMarteau, D. D.; Foropoulos, J.; Schrobilgen, G. J., unpublished results) and is even more shielded than that of $Xe[N(SO_2F)_2]_2$: −2444 ppm in SO_2ClF at 8 °C.

Table I. NMR Parameters for Xe[N(SO$_2$F)$_2$]$_2$ and F[XeN(SO$_2$F)$_2$]$_2$$^+AsF_6$$^-$ Solutions in SO$_2$ClF

				chem shift, δ[a]			coupling const, *J*, Hz	
solute[b]	solvent	temp, °C	molecule	^{129}Xe	^{15}N	^{19}F	^{129}Xe–^{15}N	^{129}Xe–^{19}F
Xe[N(SO$_2$F)$_2$]$_2$/FXeN(SO$_2$F)$_2$ mixture	SO$_2$ClF	−40	Xe[N(SO$_2$F)$_2$]$_2$	−2257	−232.5	60.2	259[c]	
			FXeN(SO$_2$F)$_2$	−2009	−247.9	−126.0 (F on Xe)	307[c]	5664
			[N(SO$_2$F)$_2$]$_2$[d]		−212.3	58.0 (F on S)		
F[XeN(SO$_2$F)$_2$]$_2$$^+AsF_6$$^-$[e]	SO$_2$ClF	−50[f]	Xe[N(SO$_2$F)$_2$]$_2$	−2248		60.3		
			i	−1878		62.2		
		−76[g]	AsF$_6$$^-$			−57.5		
		−118[h]	*h*			−259.5 (F on Xe)		
F[XeN(SO$_2$F)$_2$]$_2$$^+AsF_6$$^-$	BrF$_5$	−59	*j*	−1955	−261.7	61.1		

[a] The chemical shift convention is that outlined by IUPAC (*Pure Appl. Chem.* **1972**, *29*, 627; **1976**, *45*, 217); i.e., a positive chemical shift denotes a positive frequency and vice versa with respect to the reference substance. The following external reference substances were used: ^{129}Xe, neat XeOF$_4$ at 24 °C; ^{15}N, neat CH$_3$NO$_2$ at 24 °C, $\delta_{^{15}\mathrm{N}}$(with respect to 7.1 M aqueous NH$_4$Cl) = $\delta_{^{15}\mathrm{N}}$(with respect to CH$_3$NO$_2$) −359.7; ^{19}F, neat CFCl$_3$. [b] 30% ^{15}N enrichment. [c] The reduced coupling constants $^1K_{\mathrm{Xe-N}}$ for FXeN(SO$_2$F)$_2$ and Xe[N(SO$_2$F)$_2$]$_2$ are 9.13×10^{21} and 7.70×10^{21} N A^{-2} m^{-3}, respectively, where

$$^1K_{\mathrm{Xe-N}} = \frac{4\pi^2}{h\gamma_{^{15}\mathrm{N}}\gamma_{^{129}\mathrm{Xe}}}\,{}^1J_{^{129}\mathrm{Xe}-^{15}\mathrm{N}}$$

[d] Decomposition product formed by warming an SO$_2$ClF solution of FXeN(SO$_2$F)$_2$ and Xe[N(SO$_2$F)$_2$]$_2$ to room temperature (see Figure 2). [e] The spectrum was recorded for a freshly prepared, unwarmed solution. Warming results in an initial increase in the Xe[N(SO$_2$F)$_2$]$_2$ lines and decrease in the exchange-averaged lines in both the ^{129}Xe and the ^{19}F spectra. Lines due to [N(SO$_2$F)$_2$]$_2$ and SO$_2$F$_2$ increased in intensity in the ^{19}F spectrum as the components of eq 3–6, which contain N(SO$_2$F)$_2$ groups, decomposed upon warming to room temperature. [f] ^{129}Xe NMR spectrum. [g] ^{19}F NMR spectrum. [h] ^{19}F NMR spectrum, tentatively assigned to either XeF$^+$ or FXeF---XeN(SO$_2$F)$_2$$^+$. This resonance was observed in only low concentrations in the low-temperature ^{19}F spectra of supercooled samples that had been partially decomposed by warming to room temperature. [i] Exchange-averaged lines resulting from equilibria 3–7. [j] Exchange-averaged lines resulting primarily from equilibrium 1.

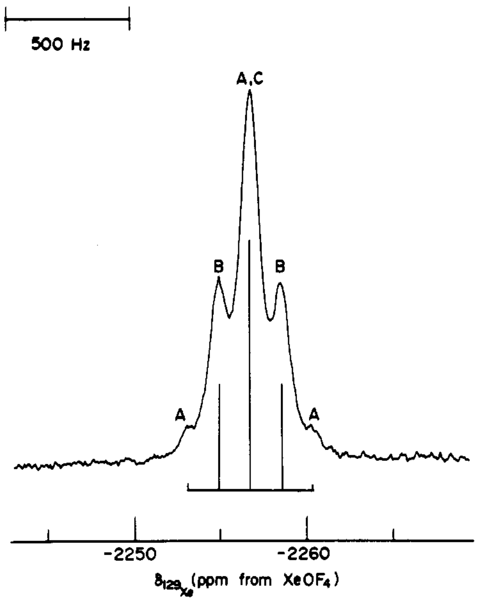

Figure 1. ^{129}Xe NMR spectrum of 30% ^{15}N-enriched Xe[N(SO$_2$F)$_2$]$_2$ recorded in SO$_2$ClF solvent at −40 °C and B_0 = 5.8719 T. Individual multiplet lines are assigned to the following isotopic isomers: (A) (FO$_2$S)$_2$^{15}NXe^{15}N(SO$_2$F)$_2$; (B) (FO$_2$S)$_2$^{14}NXe^{15}N(SO$_2$F)$_2$; (C) (FO$_2$S)$_2$^{14}NXe^{14}N(SO$_2$F)$_2$. The sum of the calculated singlet, doublet, and triplet intensities is represented by the stick diagram.

with an effective group electronegativity that is less than that for any one of these ligands.

The ^{15}N NMR spectrum of a mixtue of Xe[N(SO$_2$F)$_2$]$_2$, FXeN(SO$_2$F)$_2$, and the decomposition product, [N(SO$_2$F)$_2$]$_2$, in SO$_2$ClF solvent (−40 °C) recorded at high field strength (9.3950 T) is depicted in Figure 2. Small amounts of [N(SO$_2$F)$_2$]$_2$ observed in these samples arise from decomposition according to eq 1. The ^{15}N NMR spectra of both [N(SO$_2$F)$_2$]$_2$ and FXeN(SO$_2$F)$_2$ have been reported previously in BrF$_5$ solvent (−58 °C)[2,3] at the same field strength (9.3950 T) and are assigned in the present work on the basis of their chemical shifts in BrF$_5$ solvent. In the case of FXeN(SO$_2$F)$_2$, ^{129}Xe satellites were observed in the latter solvent but were not observed in SO$_2$ClF solvent. In contrast, ^{129}Xe satellites observed in the ^{15}N spectrum of Xe[N(SO$_2$F)$_2$]$_2$ in SO$_2$ClF solvent were assigned on the basis of the ^{129}Xe–^{15}N coupling constant measured previously in the ^{129}Xe spectrum. The high-frequency position of the ^{15}N resonance of Xe[N(SO$_2$F)$_2$]$_2$ relative to that of FXeN(SO$_2$F)$_2$ supports our earlier conclusions, based on the ^{129}Xe chemical shifts, that the Xe–N bonds are more covalent and shorter in the bis compound.

$$\mathrm{Xe[N(SO_2F)_2]_2} \rightarrow \mathrm{Xe} + \mathrm{[N(SO_2F)_2]_2} \qquad (1)$$

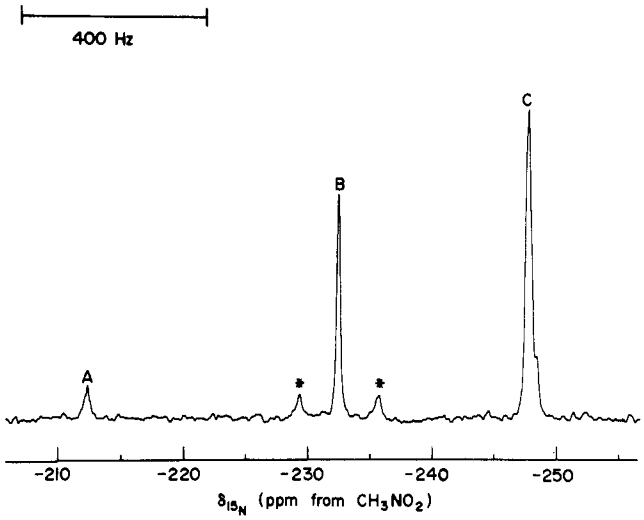

Figure 2. ^{15}N NMR spectrum of a 30% ^{15}N-enriched FXeN(SO$_2$F)$_2$ and Xe[N(SO$_2$F)$_2$]$_2$ mixture recorded in SO$_2$ClF solvent at −40 °C and B_0 = 9.3950 T. The peak assignments are as follows: (A) decomposition product, [N(SO$_2$F)$_2$]$_2$; (B) Xe[N(SO$_2$F)$_2$]$_2$; (C) FXeN(SO$_2$F)$_2$. Asterisks denote ^{129}Xe satellites.

Table II. Xenon-129 NMR Line Widths for $FXeN(SO_2F)_2$ at Variable Applied Field

B_0, T[a]	$\omega_{1/2}$, s^{-1} [b]	$B_0{}^2/\omega_{1/2}$, T^2 s
2.1139	16	0.28
5.8719	120	0.287
9.3950	333	0.265

[a] Applied field in tesla. [b] ^{129}Xe line width at half-height recorded at 24 °C.

In the case of $FXeN(SO_2F)_2$ we have noted that the ^{15}N NMR spectra exhibited ^{129}Xe satellites in BrF_5 solvent (−58 °C) but not in SO_2ClF solvent (−40 °C) at 9.3950 T. In addition, a ^{129}Xe NMR spectrum of the same sample in SO_2ClF (−40 °C) at 5.8719 T showed clearly resolved ^{129}Xe–^{15}N coupling. It must be concluded that the lack of ^{129}Xe satellites in the ^{15}N spectrum of $FXeN(SO_2F)_2$ in SO_2ClF solvent in large measure arises from shielding anisotropy (SA) relaxation. The SA mechanisn is dominant at high field strengths for a heavy nucleus such as ^{129}Xe, and its effect increases with the square of the applied field. In the extreme narrowing case and for axial symmetry, the SA contribution to the relaxation is given by eq 2.[10] It can be seen from eq 2 that the SA contribution is likely to increase for the more highly anisotropic molecule $FXeN(SO_2F)_2$ ($\Delta\sigma$ term), at low temperatures and in a more viscous solvent (τ_c increases). The solvent effect may be attributed to a greater molecular correlation time, τ_c, for $FXeN(SO_2F)_2$ in SO_2ClF than in BrF_5. In order to confirm the dominant role of SA in the relaxation of the ^{129}Xe–^{15}N coupling in $FXeN(SO_2F)_2$, the effects of SA were investigated for the ^{129}Xe resonance of the compound in BrF_5 (−58 °C) at B_0 = 2.1139, 5.8719, and 9.3950 T. The ^{129}Xe line width, $\omega_{1/2}$, should be approximately equal to $(\pi T_{1(^{129}Xe)})^{-1}$, which is, in turn, proportional to $B_0{}^2$. Close agreement among the $B_0{}^2/\omega_{1/2}$ ratios (Table II) supports the view that SA relaxation of ^{129}Xe in $FXeN(SO_2F)_2$ is dominant.

$$T_{1(^{129}Xe)}{}^{-1} = {}^{2}\!/_{15}(\sigma_{^{129}Xe})^2 B_0{}^2(\sigma_{\parallel} - \sigma_{\perp})^2\tau_c = {}^{6}\!/_{7}T_{2(^{129}Xe)}{}^{-1} \qquad (2)$$

$[^{15}N]$-$F[XeN(SO_2F)_2]_2{}^+AsF_6{}^-$. In an effort to characterize the title cation more fully, the ^{15}N and ^{129}Xe spectra were recorded in both BrF_5 and SO_2ClF media. Only a single resonance was observed for both nuclei in BrF_5 solution. These findings concur with previous ^{19}F results which report a single fluorine-on-sulfur resonance in addition to that for $AsF_6{}^-$ and the solvent. No bridging fluorine resonance was observed. It was concluded that a rapid chemical exchange process was responsible for the ^{19}F results,[4] and this is supported by the present ^{15}N and ^{129}Xe findings. The following dissociative equilibrium appears to explain both sets of findings:

$$F[XeN(SO_2F)_2]_2{}^+ \rightleftarrows FXeN(SO_2F)_2 + XeN(SO_2F)_2{}^+ \qquad (3)$$

However, dissolution in SO_2ClF and study by ^{129}Xe NMR spectroscopy (the ^{15}N spectra could not be obtained owing to low solubility of the compound) revealed a broad line ($\omega_{1/2}$ = 750 Hz) at −1882 ppm and a high-field line corresponding to $Xe[N(SO_2F)_2]_2$ having the chemical shift and fine structure depicted in Figure 1. In the lower dielectric medium, SO_2ClF, the dissociation and resulting exchange processes associated with $F[XeN(SO_2F)_2]_2{}^+$ also apparently involve covalent species. The identification of one such species, $Xe[N(SO_2F)_2]_2$, suggests that equilibrium 4 is also an important dissociation process. The rapid chemical exchange responsible for the broad, high-frequency ^{129}Xe line at −1882 ppm presumably occurs by exchange of fluorine bonded to xenon. Thus, only the ionic components of equilibria 3 and 4 participate in the exchange process represented by equilibria 5–7. The high-frequency position and line width of the −1882-ppm line is consistent with chemical exchange among $F[XeN(SO_2F)_2]_2{}^+$, $FXeN(SO_2F)_2$, $XeN(SO_2F)_2{}^+$, XeF_2, XeF^+, and $Xe_2F_3{}^+$.[7] All of these possess or would be expected to possess ^{129}Xe chemical shifts to significantly lower field than that of $Xe[N(SO_2F)_2]_2$.

$$F[XeN(SO_2F)_2]_2{}^+ \rightleftarrows Xe[N(SO_2F)_2]_2 + XeF^+ \qquad (4)$$

$$FXeN(SO_2F)_2 + {}^*XeN(SO_2F)_2{}^+ \rightleftarrows F^*XeN(SO_2F)_2 + XeN(SO_2F)_2{}^+ \qquad (5)$$

$$FXeN(SO_2F)_2 + XeF^+ \rightleftarrows XeF_2 + XeN(SO_2F)_2{}^+ \qquad (6)$$

$$XeF^+ + XeF_2 \rightleftarrows Xe_2F_3{}^+ \qquad (7)$$

Freshly prepared samples of $F[XeN(SO_2F)_2]_2{}^+$ dissolved in SO_2ClF yielded a spectrum with a single fluorine-on-sulfur resonance (62.2 ppm) at −76 °C. Brief warming to room temperature (ca. 5 s) followed by rapid quenching yielded a second fluorine-on-sulfur resonance (60.3 ppm), which may be associated with $Xe[N(SO_2F)_2]_2$, while the former resonance must be associated with exchange-averaged contributions of $FXeN(SO_2F)_2$ and $XeN(SO_2F)_2{}^+$. Further warming enhanced the 60.3-ppm peak and generated a new peak at 58.0 ppm. The latter is assigned to $[N(SO_2F)_2]_2$, which presumably arises from reductive eliminations of xenon gas such as represented by eq 1 and 8.

$$2FXeN(SO_2F)_2 \rightarrow XeF_2 + [N(SO_2F)_2]_2 + Xe \qquad (8)$$

Brief cooling of warmed samples to −118 °C yielded supersaturated solutions which revealed a low-frequency signal in the fluorine-on-xenon(II) region of the spectrum with accompanying ^{129}Xe satellites. This signal was exchange averaged at −76 °C and found to be absent in unwarmed samples cooled to −188 °C. In addition, the fluorine bridge resonance of $Xe_2F_3{}^+$ occurs at −184.7 ppm ($J_{^{129}Xe-^{19}F}$ = 4865 Hz) in BrF_5[11] compared to −259.5 ppm ($J_{^{129}Xe-^{19}F}$ = 6604 Hz) for the new line, eliminating the as yet unobserved bridging fluorine resonance of $F[XeN(SO_2F)_2]_2{}^+$ as a possibility. The low-frequency position and large xenon–fluorine coupling constant also eliminate the possibility that the new resonance arises from either free XeF_2 (−180 ppm, $J_{^{129}Xe-^{19}F}$ = 5621 Hz; SO_2ClF solvent)[7] or $FXeN(SO_2F)_2$ (−126.0 ppm, $J_{^{129}Xe-^{19}F}$ = 5564 Hz; SO_2ClF solvent)[2,3] generated in eq 3, 5, and 6. It is possible that the new fluorine resonance is due to XeF_2 weakly coordinated through a fluorine bridge. Previous examples of such compounds containing weakly fluorine-bridged XeF_2 molecules include $FXeF{-}{-}{-}WOF_4$,[12] $FXeF{-}{-}{-}MoOF_4$,[12] and $XeF_2{\cdot}BrOF_2{}^+$.[13] It is possible that the resonance may be attributed to the $FXeF{-}{-}{-}XeN(SO_2F)_2{}^+$ cation, which is analogous to the $FXeF{-}{-}{-}XeOTeF_5{}^+$ [13] cation previously identified in BrF_5 solution. In the last three examples Xe–F bonds are deemed to be rendered equivalent on the NMR time scale by rapid breaking and remaking of the weaker Xe-F bridge bond. Alternatively, the new line may be assigned to the XeF^+ cation, which has been shown to have ^{19}F chemical shifts ranging from −245.5 ppm ($J_{^{129}Xe-^{19}F}$ = 6710 Hz) in HSO_3F to −290.2 ppm ($J_{^{129}Xe-^{19}F}$ = 7230 Hz) in SbF_5.[11] The latter cation could presumably arise by means of the following decomposition when solutions are warmed to room temperature:

$$F[XeN(SO_2F)_2]_2{}^+ \rightarrow XeF^+ + [N(SO_2F)_2]_2 + Xe \qquad (9)$$

Raman Spectrum of $Xe[N(SO_2F)_2]_2$. In the absence of an X-ray crystal structure, it is not possible to unambiguously assign a molecular point group to $Xe[N(SO_2F)_2]_2$. A multitude of possible conformational isomers arise from combinations of rotational orientations about the Xe–N and S–N bonds and result in several possible molecular point symme-

---

(10) Webb, G. A. In ref 7, Chapter 3.

(11) Gillespie, R. J.; Netzer, A.; Schrobilgen, G. J. *Inorg. Chem.* **1974**, *13*, 1455.

(12) Holloway, J. H.; Schrobilgen, G. J. *Inorg. Chem.* **1980**, *19*, 2632.

(13) Keller, N.; Schrobilgen, G. J. *Inorg. Chem.* **1981**, *20*, 2118.

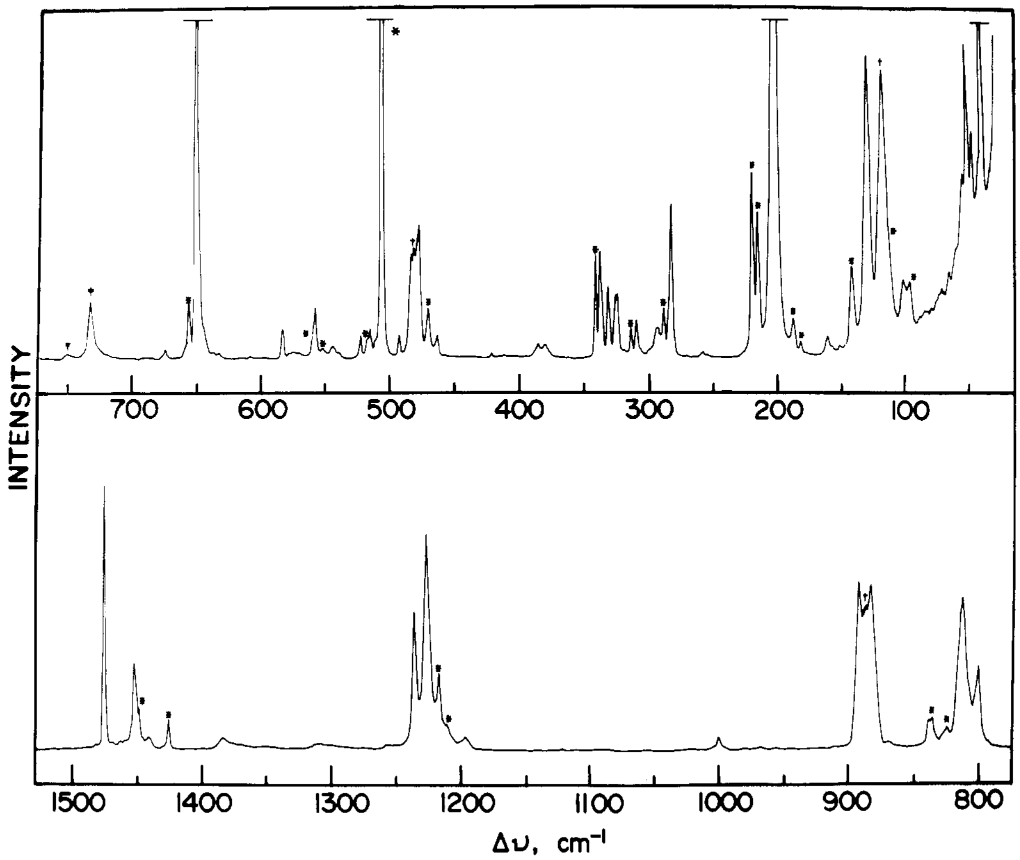

Figure 3. Raman spectrum of $Xe[N(SO_2F)_2]_2$ recorded at −196 °C with 5145-Å excitation. The sample contained unreacted $FXeN(SO_2F)_2$, whose lines are denoted by asterisks. Coincidences between $Xe[N(SO_2F)_2]_2$ and $FXeN(SO_2F)_2$ lines are denoted by daggers; FEP sample tube lines are denoted by double daggers.

Table III. Raman Frequencies and Tentative Assignments for $Xe[N(SO_2F)_2]_2$ Compared to Those for $FXeN(SO_2F)_2$[a]

freq, cm^{-1}		
$Xe[N(SO_2F)_2]_2$	$FXeN(SO_2F)_2$[b]	approx descripn
1476 (21), 1452 (7)	1451 (14), 1449 (24)	SO_2 asym str, i
1441 (1)	1439 (2), 1425 (19)	SO_2 asym str, o
1257 (1), 1236 (10)	1223 (19), 1216 (20)	SO_2 sym str, i
1227 (18), 1196 (1)	1209 (10), 1206 sh	SO_2 sym str, o
891 (15), 882 (16)	888 (33), 881 (11)	SNS asym str
837 (3)	842 (4), 836 (13)	SF str, i and o
810 (13), 806 sh, 798 (7)	797 (23), 825 (17)	SNS sym str
674 (1), 649 (40), 643 sh	656 (41)	SO_2 bend, o
583 (3)	581 (9)	SO_2 ⊥ rock, o
560 sh, 557 (5), 544 (1)	559 (8), 551 (7)	SO_2 ⊥ rock, i
522 (1), 517 sh, 515 (3), 492 (2)	514 (6)	SO_2 bend, i
	506 (100)	XeF str
483 (9), 481 (11), 477 (14)	478 (17)	SO_2 ∥ rock, i and o
463 (2)	469 (17)	SF ∥ wag, i and o
413 (0.5), 406 (0.2)	422 (4)	XeN sym str
386 (2), 380 (2)		XeN asym str
338 (11), 331 (8)	340 (52)	SNS bend
326 (5), 324 (5), 316 (1), 309 (4)	312 (18)	SF ⊥ wag, i and o
293 (4), 284 sh, 282 (16)	286 (22)	SO_2F torsion, i and o
	220 (113), 215 (87)	FXeN ∥ bend
	186 (13), 180 (7)	FXeN ⊥ bend
201 (100)		NXeN ∥ bend
161 (3)		NXeN ⊥ bend
152 (2)		$N(SO_2F)_2$ torsion
	141 (43)	lattice mode
130 (32)	119 (28), 116 (27)	XeNS ∥ bend
118 (29)	111 (31), 96 (22)	XeNS ⊥ bend
101 (5), 85 (1), 79 (1), 71 (1), 65 (1), 55 (8)	87 (6), 60 sh, 56 (16), 55 sh, 50 (111), 46 (57)	lattice modes

[a] The Raman spectrum of $Xe[N(SO_2F)_2]_2$ was recorded in an FEP sample tube at −196 °C with use of the 5145-Å exciting line. Values in parentheses denote intensities. Abbreviations: i, in-phase vibrations; o, out-of-phase vibrations (attributed to coupling of SO_2F group modes in the same $N(SO_2F)_2$ group); ∥, parallel to the SNS plane; ⊥, perpendicular to the SNS plane; sh, shoulder. [b] Reference 3.

tries, namely, D_{2h}, D_2, C_{2v}, C_{2h}, C_2, C_s, C_i, and C_1. A cursory examination of the Raman vibrational data indicates 46 bands (excluding lattice modes) attributable to $Xe[N(SO_2F)_2]_2$ (Figure 3 and Table III). Of the point group possibilities cited above, all those possessing a center of inversion at xenon give rise to 24 Raman bands, i.e. D_{2h}, C_{2h}, and C_i, while D_2, C_{2v},

C_2, C_s, and C_1 would give rise to 51 Raman bands. Both values are derived from the assumption that vibrational coupling occurs between the modes of the $N(SO_2F)_2$ groups. The preceding analysis apparently eliminates point groups containing an inversion center. For the purposes of the present assignments, the most favorable conformation not possessing a center of symmetry is one in which the two SNS planes are staggered and the orientations of SO_2F groups are the same as the relative orientations of SO_2F groups deduced from the crystal structure of $FXeN(SO_2F)_2$ (C_2 molecular symmetry, i.e., fluorines being trans with respect to their SNS plane).[3] This conformation belongs to the point group D_2, and the Raman spectrum may be assigned accordingly. Thus, $\Gamma_{\mathrm{vib}} = 13\ \mathrm{A} + 12\ \mathrm{B}_1 + 13\ \mathrm{B}_2 + 13\ B_3$ and all 51 modes are expected to be Raman active ($12\ \mathrm{B}_1 + 13\ \mathrm{B}_2 + 13\ \mathrm{B}_3$ are infrared active) under the proposed D_2 symmetry for $Xe[N(SO_2F)_2]_2$.

As in $FXeN(SO_2F)_2$,[3] nine vibrations may be attributed to the SO_2F group: SO_2 symmetric and asymmetric stretches, an SO_2 bend, two SO_2 rocks, an SF stretch, two SF wags, and an SO_2F torsion (the SO_2 rocking and SF wagging vibrations can occur parallel or perpendicular to the SNS plane). Each of these vibrations gives rise to two lines in the spectrum (with intramolecular coupling between $N(SO_2F)_2$ groups ignored) which are regarded as arising from coupling between the two SO_2F groups of each $N(SO_2F)_2$ group and are described as in-phase and out-of-phase motions of these groups. These in-phase and out-of-phase motions may in turn couple with those of the other $N(SO_2F)_2$ group, accounting for 36 modes. Three vibrations may be assigned to the SNS bridging group: a symmetric stretch, an asymmetric stretch, and a bend that, with coupling, yields an additional six modes. Finally, the linear N–Xe–N group is expected to contribute six vibrations: two stretches, Xe–N symmetric and asymmetric stretches, and four bends, in the SNS plane and out of the SNS plane N–Xe–N and Xe–N–S bends. The Xe–N–S bends associated with the two $N(SO_2F)_2$ groups also couple, yielding two additional modes. Finally, the single remaining mode is the result of torsional motions of the two $N(SO_2F)_2$ groups relative to each other.

Although the vibrational spectrum of an $FXeN(SO_2F)_2$–$Xe[N(SO_2F)_2]_2$ mixture has been reported recently,[4] no detailed assignments of the frequencies have been attempted. Tentative assignments for the Raman spectrum of $Xe[N(SO_2F)_2]_2$ are given in Table III and are compared to those for $FXeN(SO_2F)_2$, which have been reported earlier.[3] Details relating to the assignments of the modes of the SO_2F and SNS groups, which have been assigned by analogy with those of $FXeN(SO_2F)_2$, can be found in ref 3. The Xe–N stretches are tentatively assigned to weak lines in the 380–415-cm^{-1} region, in agreement with the Xe–N stretch of $FXeN(SO_2F)_2$, which was observed at 422 cm^{-1} and its assignment confirmed by ^{15}N isotopic enrichment.[3] The N–Xe–N bends are assigned at lower frequencies than those of their F–Xe–N counterparts in $FXeN(SO_2F)_2$. Both the parallel N–Xe–N and F–Xe–N bends in the molecules are responsible for the most intense bands in their respective spectra. The assignment of the $N(SO_2F)_2$ torsion is highly tentative but is expected to occur at a significantly lower frequency than SO_2F torsional modes.

Experimental Section

Apparatus and Materials. All manipulations involving air-sensitive materials were carried out under anhydrous conditions on vacuum lines constructed from 316 stainless steel, nickel, Teflon, FEP, and Kel-F and/or in a drybox. Arsenic pentafluoride, SO_2ClF, BrF_5, and CF_2Cl_2 were transferred under vacuum through FEP, Kel-F, and/or Teflon connections. Air-sensitive substances of low volatility, i.e., XeF_2, $[^{15}N]$-$HN(SO_2F)_2$, and $[^{15}N]$-$FXeN(SO_2F)_2$, were transferred in a drybox.

Bromine pentafluoride (Matheson),[13] SO_2ClF (Columbia Organic Chemicals),[12] and CF_2Cl_2 (Matheson)[3] were purified by the standard literature methods. The preparations of AsF_5,[13] XeF_2,[14] $[^{15}N]$-$HN(SO_2F)_2$,[3] and $[^{15}N]$-$FXeN(SO_2F)_2$[3] have been described elsewhere.

Preparation of $[^{15}N]$-$Xe[N(SO_2F)_2]_2$. Nitrogen-15-enriched $Xe[N(SO_2F)_2]_2$ was prepared according to the reaction

$$[^{15}N]\text{-}FXeN(SO_2F)_2 + [^{15}N]\text{-}HN(SO_2F)_2 \xrightleftharpoons[CF_2Cl_2]{-15\text{ to }-12\ ^\circ C} [^{15}N]\text{-}Xe[N(SO_2F)_2]_2 + HF \quad (10)$$

In a typical preparation, 0.219 g (1.21 mmol) of 30% ^{15}N-enriched $HN(SO_2F)_2$ was syringed onto 0.365 g (1.10 mmol) of 30% ^{15}N-enriched $FXeN(SO_2F)_2$ in an FEP vessel (cooled to −196 °C in a drybox). After the cold reaction vessel was equipped with a Kel-F valve, 4 mL of CF_2Cl_2 (previously dried over P_2O_5) was condensed onto the sample at −196 °C and the sample warmed to −15 to −12 °C in an ice–salt bath and vigorously agitated every 4–8 h. After 24 h, the solvent and HF produced were removed under vacuum at the ice–salt bath temperature and replenished with 4 mL of fresh CF_2Cl_2. The reaction was allowed to proceed for 3 days before the solvent was finally removed. In all preparations, the product was found to still contain unreacted $[^{15}N]$-$HN(SO_2F)_2$ and $[^{15}N]$-$FXeN(SO_2F)_2$ (ca. 20% under optimum conditions). Unreacted $[^{15}N]$-$HN(SO_2F)_2$ and $[^{15}N]$-$[N(SO_2F)_2]_2$ decomposition product were effectively removed by pumping at −10 to 0 °C for several hours. The resulting white solid was examined in situ by low-temperature Raman spectroscopy. NMR samples were prepared by maintaining the bulk sample at −196 to −80 °C and transferring into a precision glass NMR tube previously cooled to −196 °C in a drybox. The sample was maintained cold and dissolved in SO_2ClF at −40 to −20 °C prior to recording NMR spectra at −40 °C.

Preparation of $[^{15}N]$-$F[XeN(SO_2F)_2]_2^+AsF_6^-$. The title compound was prepared according to eq 11. In a typical preparation, 2.546

$$2[^{15}N]\text{-}FXeN(SO_2F)_2 + AsF_5 \xrightarrow{-78\text{ to }+25\ ^\circ C} [^{15}N]\text{-}F[XeN(SO_2F)_2]_2^+AsF_6^- \quad (11)$$

g (7.705 mmol) of 30% ^{15}N-enriched $FXeN(SO_2F)_2$ was placed in an FEP reaction vessel equipped with a Kel-F valve. A 10-fold excess of AsF_5 was condensed onto the sample at −78 °C and maintained at this temperature for 8 h. The partially reacted sample was then slowly warmed to room temperature, and the excess AsF_5 was allowed to expand into the vacuum manifold and adjusted to a total pressure of 1600 torr at room temperature. The sample pressure was periodically readjusted to 1600 torr as the reaction proceeded over the next $^1/_2$ h. The AsF_5 was recondensed, wetting the entire sample, and warmed as above. The condensation–warming cycle was repeated a total of three times before the sample was allowed to stand under 1600 torr of AsF_5 at room temperature for an additional 1 h. The sample was then evacuated at room temperature and pumped on until AsF_5 no longer evolved from the sample. Mass measurements confirmed the stoichiometry represented by eq 11, i.e., 3.154 g (3.800 mmol) compared to the theoretical quantities, 3.200 g (3.853 mmol). The light yellow compound was found to be stable at room temperature but was stored at −78 °C under a positive pressure of dry N_2 gas until used.

Laser Raman Spectroscopy. A Spectra-Physics Model 164 argon ion laser, giving up to 900 mW at 5145 Å, was used to excite the Raman spectra. The spectrometer was a Spex Industries Model 14018 double monochromator equipped with 1800 grooves/mm holographic gratings. The spectrometer was periodically calibrated by recording the discharge lines from an argon lamp over the spectral range of interest; the Raman shifts quoted are estimated to be accurate to ±1 cm^{-1}. Slit widths depended on the scattering efficiency of the sample, laser power, etc., with 1.0 cm^{-1} being typical.

FEP ($^1/_4$ in. o.d. x 1/32 wall) sample tubes were mounted vertically. The angle between the incident laser beam and the sample tube was 45°, and Raman scattered radiation was observed at 45° to the laser beam (90° to the sample tube axis).

Low-temperature spectra were recorded at −196 °C by mounting the sample vertically in an unsilvered Pyrex glass Dewar filled with liquid nitrogen.

Nuclear Magnetic Resonance. All spectra were recorded on pulse spectrometers and accumulated in 16K (^{15}N, ^{19}F) or 32K (^{129}Xe) of memory. All ^{19}F spectra were obtained with an external deuterium

---

(14) Williamson, S. M. *Inorg. Synth.* **1968**, *11*, 147.

Inorg. Chem. **1983**, *22*, 2183-2187

lock; ^{15}N and ^{129}Xe spectra were obtained on instruments equipped with superconducting magnets and were run unlocked. Fluorine-19 spectra were obtained on a Bruker WH-90 spectrometer at 84.66 MHz in 100–600 scans with a spectral width of 25 kHz (3.0 Hz/data point, pulse acquisition time 0.327 s) and a pulse width of 2 μs. Xenon-129 spectra were obtained at 69.20 MHz on a Bruker WM-250 in 10000–20000 scans at spectral widths of 100 kHz (6.1 Hz/data point, pulse acquisition time 0.164 s and pulse width 20 μs). Nitrogen-15 spectra were obtained at 40.55 MHz on a Bruker WH-400 spectrometer in 200–400 scans. The spectral width was 20 kHz (2.4 Hz/data point, pulse acquisition time 0.410 s) with a pulse width of 30 μs. The pulse widths cited correspond to tip angles, θ, of ~90° for ^{19}F and ^{129}Xe and ~30° for ^{15}N. A relaxation delay time of 15 s was used in the accumulation of ^{15}N data; a zero relaxation delay was applied to ^{19}F and ^{129}Xe spectral accumulations. Line-broadening parameters used in exponential multiplication of the free induction decays were set equal to their respective data point resolutions. All spectra were obtained with precision thin-walled glass NMR tubes (Wilmad) of 5 mm o.d. (^{19}F) and 10 mm o.d. (^{15}N and ^{129}Xe).

Variable-temperature studies were carried out with use of Bruker temperature controllers. Temperatures were measured with a copper–constantan thermocouple inserted directly into the sample region of the probe and were accurate to ±1 °C.

Acknowledgment. We thank Natural Sciences and Engineering Research Council of Canada for financial support and the Southwest Ontario Regional NMR Center, Guelph, Ontario, for recording the ^{15}N NMR spectra reported in this work.

Registry No. $Xe[N(SO_2F)_2]_2$, 85883-06-3; $FXeN(SO_2F)_2$, 53719-78-1; $HN(SO_2F)_2$, 14984-73-7; $F[XeN(SO_2F)_2]_2{}^+AsF_6{}^-$, 85883-05-2; AsF_5, 7784-36-3.

Contribution from the Institut für Anorganische und Analytische Chemie der Freien Universität Berlin,
D-1000 Berlin 33, West Germany

Tellurium–Nitrogen Compounds

HANS HARTL, PETER HUPPMANN, DIETER LENTZ, and KONRAD SEPPELT*

Received September 10, 1982

With H_2N-TeF_5 and $(CH_3)_3SiNHTeF_5$ as the starting materials numerous new tellurium–nitrogen compounds have been synthesized. Almost all of them contain the $>N-TeF_5$ group, which stabilizes many double-bonded systems such as $O=C=NTeF_5$ and $Cl_4W=NTeF_5$. $Cl_2Se=NTeF_5$ is a rare example of a compound containing a discrete selenium–nitrogen double bond.

Introduction

The chemistry of sulfur–nitrogen compounds is a vast and still expanding field. Quite in contrast very little is known about selenium–nitrogen systems. Even less is known about the system tellurium–nitrogen: not even a well-defined binary compound is known. But it was shown that TeF_6 can act as a source of tellurium–nitrogen compounds, and derivatives such as $(CH_3)_2NTeF_5$,[1,2] $(CH_3)_3SiNHTeF_5$,[3] and H_2NTeF_5[3] were prepared.

By comparison with H_2NSF_5,[4] H_2NTeF_5 turned out to be more stable against HF elimination and to be less basic, and the TeF_5 group to be probably more electron withdrawing than the SF_5 group. In this paper we describe a large number of new compounds that have been obtained by reaction with H_2NTeF_5 and/or $(CH_3)_3SiNHTeF_5$.

Experimental Section

General Considerations. Fluorine NMR spectra were taken on a Varian 360 instrument with standard 5 mm o.d. glass tubes and with $CFCl_3$ as internal or external reference.

Infrared spectra were recorded on a Beckman 11 spectrometer; the window material most commonly used was KCl.

Raman spectra were taken on a Coderg PH 1 instrument using a He–Ne laser for excitation (190 mW).

Mass spectra were taken on a Varian MAT 5 instrument with 70 eV excitation energy.

Reagents. SF_4, PF_5, MoF_6, and $(CH_3)_3SiBr$ were commercially available. ClF,[5] SOF_4,[6] COF_2,[7] SeF_4,[8] $SeCl_4$,[9] and WCl_6[10] were prepared according to literature methods.

Preparation of ((Trimethylsilyl)amino)tellurium Pentafluoride and *cis*-Bis((trimethylsilyl)amino)tellurium Tetrafluoride. *Caution*: *cis*-$[(CH_3)_3SiNH]_2TeF_4$ is explosive! The reaction of TeF_6 (0.1 mol) and $[(CH_3)_3Si]_2NH$ (0.1 mol) in a stainless steel cylinder affords over 90% yields of $(CH_3)_3SiNHTeF_5$,[3] if the cylinder has been cleaned thoroughly prior to use with concentrated nitric acid and if the reaction is run with magnetic stirring for 1 week at room temperature. The volatile contents of the cylinder are trapped at −196 °C and fractionally distilled under vacuum through a −30 °C trap. Under these conditions almost no *cis*-$[(CH_3)_3SiNH]_2TeF_4$ is formed. For the physical data of $(CH_3)_3SiNHTeF_5$, see ref 3.

The formation of *cis*-$[(CH_3)_3SiNH]_2TeF_4$ occurs if the same starting materials are reacted at elevated temperature, especially above 60 °C, or if the stainless steel cylinder has not been cleaned between two runs. Our observations point in the direction that the formation of *cis*-$[(CH_3)_3SiNH]_2TeF_4$ is autocatalytic.

Pure $(CH_3)_3SiNHTeF_5$ was distilled several times at 58 °C (19 mbar), but once it decomposed spontaneously into TeF_6 and *cis*-$[(CH_3)_3SiNH]_2TeF_4$.

Since the bis compound turned out to be explosive, no further attempts for its preparation were made. Crude material has been purified by sublimation at 40 °C (10^{-3} mbar). When it is heated to 100 °C, it decomposes with mild explosions. It is a colorless, crystalline solid, and its structure was resolved by NMR spectroscopy.

^{19}F NMR (in CH_2Cl_2): a_2b_2 spectrum, δ_a 26.9, δ_b 19.5; J_{a-b} = 133 Hz. ^{1}H NMR: δ_{CH_3} 0.55, δ_{NH} 4.4.

A 50-g amount of *cis*-$[(CH_3)_3SiNH]_2TeF_4$ was kept for $^1/_2$ yr in a glass cylinder. The material had definitely changed composition,

---

(1) Fraser, G. W.; Peacock, R. D.; Watkins, P. M. *J. Chem. Soc., Chem. Commun.* **1976**, 1248.

(2) Fraser, G. W.; Peacock, R. D.; Watkins, P. M. *J. Chem. Soc. A* **1971**, 1125.

(3) Seppelt, K. *Inorg. Chem.* **1973**, *12*, 2873.

(4) Clifford, A. F.; Duncan, L. C. *Inorg. Chem.* **1966**, *5*, 692.

(5) Schack, C. J.; Wilson, R. D. *Synth. Inorg. Met.-Org. Chem.* **1973**, *3*, 393.

(6) Seppelt, K. *Z. Anorg. Allg. Chem.* **1971**, 386, 229; *Inorg. Synth.* **1980**, *20*, 35.

(7) Tullock, C. W.; Coffman, D. D. *J. Org. Chem.* **1960**, *25*, 2016.

(8) Oppegard, A. L.; Smith, W. C.; Muetterties, E. L.; Engelhardt, V. A. *J. Am. Chem. Soc.* **1960**, *82*, 3835.

(9) Brauer, G. "Handbuch der präparativen Anorganischen Chemie"; Enke Verlag: Stuttgart, 1975; p 416.

(10) Brauer, G. "Handbuch der präparativen Anorganischen Chemie"; Enke Verlag: Stuttgart, 1981; p 1558.

0020-1669/83/1322-2183$01.50/0